Jurnal Teknologi

DESIGN OF MULIFREQUENCY ELECTRICAL IMPEDANCE TOMOGRAPHY (MfEIT) BASED ON ANALOG DISCOVERY TO DETECT BREAST CANCER

Khusnul Ain[a], Franky Chandra Satria Arisgraha[a], Nuril Ukhrowiyah[b], Imam Sapuan[b], Ade Agung Harnawan[c], Valentinus Mahendra Aaron Quendangen[a], Bayu Ariwanto[d], Inas Amira[d]

[a]Biomedical Engineering, Airlangga University, Surabaya, Indonesia
[b]Physics, Airlangga University, Surabaya, Indonesia
[c]Physics, Lambung Mangkurat University, Banjarmasin, Indoensia
[d]Megister of Biomedical Engineering, Airlangga University, Surabaya, Indoensia

Graphical Abstract
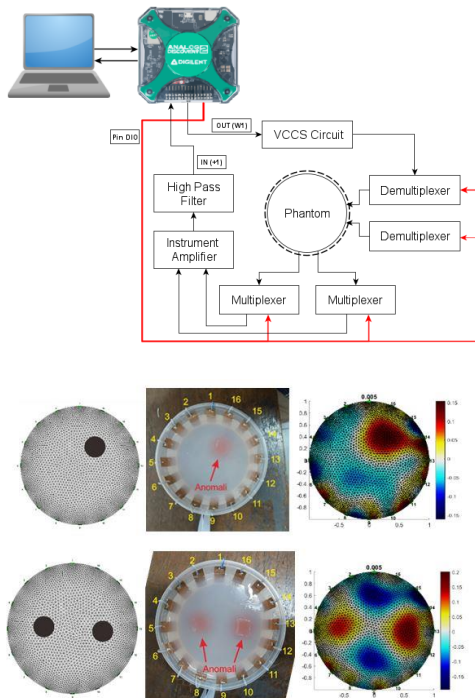
Abstract

This study aims to design Multifrequency Electrical Impedance Tomography (MfEIT) based on Analog Discovery to detect breast cancer. The MfEIT was built from Analog Discovery which can be used as a signal generator, power supply, voltage control and measuring voltage and phase difference. Other complementary modules are Multiplexer, Instrument amplifier, Voltage Constant Current Source (VCCS), and High Pass Filter (HPF). The MfEIT performance test was carried out on a phantom object made of agar with a certain conductivity that represents breast and cancer tissue. The MfEIT performance testing at a frequency of 10 kHz, 40 kHz, and 80 kHz. The reconstruction from both potential and phase difference data, it shown that are in accordance with the phantom condition, both in number, size and position of anomalies. The reconstruction from the voltage data shown fine at all frequencies, but the phase data produces a good reconstruction image when frequencies was less than 80 kHz.

Keywords: Multi frequency, electrical impedance, tomography, analog discovery, breast cancer

Abstrak

Penelitian ini bertujuan untuk merancang Multifrequency Electrical Impedance Tomography (MfEIT) berbasis Analog Discovery untuk mendeteksi kanker payudara. MfEIT dibangun dari Analog Discovery yang dapat digunakan sebagai pembangkit isyarat, catu daya, kontrol tegangan dan pengukur tegangan dan beda fasa. Modul pelengkap lainnya adalah Multiplexer, penguat instrumen, Voltage Constant Current Source (VCCS), dan High Pass Filter (HPF). Pengujian kinerja MfEIT dilakukan pada objek phantom yang terbuat dari jeli dengan konduktivitas tertentu yang merepresentasikan jaringan payudara dan kanker. Pengujian kinerja MfEIT dilakukan pada frekuensi 10 kHz, 40 kHz, dan 80 kHz. Hasil rekonstruksi dari data potensial dan beda fasa, menunjukkan bahwa hasil rekonstruksi sesuai dengan kondisi phantom, baik jumlah, ukuran maupun posisi anomali. Rekonstruksi dari data tegangan menunjukkan hasil yang baik pada semua frekuensi, namun data fase menghasilkan gambar rekonstruksi yang baik pada frekuensi kurang dari 80 kHz.

Kata kunci: frequenci ganda, tomografi, impedansi elektrik, analog discovery, kanker payudara

1.0 INTRODUCTION

Cancer is an abnormal growth of body tissue cells that become malignant, with its incidence rising. These cells can grow and spread to other body parts, potentially leading to death[1], [2]. One feared type of cancer among women is breast cancer, often detected at advanced stages [3]. According to WHO's Globocan data for 2022, the total number of breast cancer cases in Indonesia reached 68,858 (16.6%) out of 396,914 cancer cases, with 22,430 deaths (9.6%) attributed to breast cancer. Breast cancer ranks first as of the most prevalent cancer type and the leading cause of cancer-related deaths in Indonesia. Moreover, 70% of breast cancer cases are detected at advanced stages[4].

Early detection remains pivotal in improving survival rates and facilitating less invasive treatment options for breast cancer patients [1], [3]. Traditional screening methods, like mammography and ultrasound, have been instrumental in early detection efforts. However, they are not without limitations, particularly in women with dense breast tissue, where sensitivity can be reduced. Hence, there is an ongoing quest for novel and complementary diagnostic tools to enhance breast cancer detection[5]. Moreover, early detection has a significant impact on patient prognosis and recovery.

Currently, several tools using medical imaging technology have played a crucial role in the early detection of breast cancer, including ultrasonography, CT scans, X-ray mammography, ductography, xerodiography, thermography, and MRI are used for breast cancer detection (USG) [6], [7], [8]. However, mammography is the most commonly used tool for breast cancer detection and serves as the standard [8]. Nevertheless, due to its use of X-rays, mammography has limitations like ionizing radiation, patient discomfort due to breast compression, and reduced detection capabilities in dense breast tissue[9]. X-ray mammography is also not recommended for patients under 45 and pregnant women[10]. X-ray mammography is expensive and only available in major urban areas. Therefore, tools with several advantages compared to other imaging techniques, such as non-invasive, radiation-free techniques, long-term safe monitoring, portability, cost-effectiveness, and rapid imaging capability and become one emerging technology like Electrical Impedance Tomography (EIT) for breast cancer detection are more widely accepted [8], [11], [12].

EIT is an imaging technique based on changes in electrical impedance within the body's tissues [12]. The fundamental principle of EIT involves injecting small electrical current and measuring electrical potential simultaneously on the body's surface using electrodes placed on the skin [13]. By reconstructing the electrical potential properties like conductivity and permittivity [12], [14], three-dimensional images representing the electrical impedance composition of the body's tissues can be generated [12], [15], [16].

Therefore, EIT imaging is a modality with potential applications in various medical fields [17], including breast cancer diagnostics [7], [18], [19]. EIT operates by measuring the electrical impedance within biological tissues. These properties can significantly differ between healthy and cancerous tissues due to disparities in cell density, water content, and vascularization [13].

The development of EIT for breast cancer detection offers significant potential because it is non-invasive, safe, and relatively affordable. By utilizing the Analog Discovery module, which has the capability to generate multifrequency signals within a specific spectrum and measure signal phase [20], [21], EIT based on Analog Discovery can enhance its accuracy and sensitivity in breast cancer detection.

However, conventional EIT systems predominantly rely on single-frequency measurements, which have inherent limitations in spatial resolution and the ability to distinguish between various tissue types effectively [22]. Multifrequency Electrical Impedance Tomography (mfEIT) presents a promising avenue to address these challenges. MfEIT involves using multiple frequencies during measurements, offering more comprehensive information about tissue properties and potentially enhancing sensitivity and specificity in detecting breast cancer [23], [24].

To date, the application of EIT in breast cancer detection has faced technical obstacles related to system design, data acquisition, and image reconstruction. While various studies, have showcased the potential of EIT in breast cancer diagnostics [7], [8], [9], [18], the practical implementation of MfEIT systems based on readily accessible and cost-effective platforms like Analog Discovery remains an area ripe for exploration [23]. Our research seeks to bridge this gap by proposing the design and development of a Multifrequency Electrical Impedance Tomography (MfEIT) system centered around Analog Discovery, offering a unique opportunity to enhance the accuracy and accessibility of breast cancer detection through advanced electrical impedance imaging [24]. Then, the image was created using Eidors software [25], [26].

By harnessing this technology, it is hoped that a more effective imaging system for early breast cancer detection can be developed. This can help minimize patient risks, reduce treatment costs, and improve survival rates. Therefore, this research has the potential to make a significant contribution to the global effort to combat breast cancer through the use of innovative medical technology

Based on the aforementioned description, research has been conducted to design an Electrical Impedance Tomography (EIT) device for breast cancer detection, which is expected to be a more accessible and portable alternative for breast cancer detection. The study used the Analog Discovery, a breast-shaped agar phantom with anomalies. Measurements were performed at 10 kHz, 40 kHz, and 80 kHz, obtaining voltage (V) and phase (θ) data.

Based on this data, image reconstruction results were obtained using EIDORS software.

2.0 METHODOLOGY

Activities of research include: design of the MfEIT device, components that make up the MfEIT device which include generator, VCCS, multiplexer-demultiplexer, instrument amplifier, high pass filter, making breast phantoms, EIDORS, data collection and analysis.

The Digilent Waveform software driver was used to operate the Analog Discovery-based MfEIT through a USB 2.0 connection. Meanwhile, the reconstruction was carried out using EIDORS, which is based on Matlab. The schematic design of the MfEIT system based on Analog Discovery is shown Figure 1.

Analog discovery is useful for generating sinusoidal AC signals via a USB connection. Generator testing was carried out to determine its ability to generate signals from a frequency of 1 Hz to 1 MHz, the results were observed by an oscilloscope. The control flowchat is shown in Figure 2.
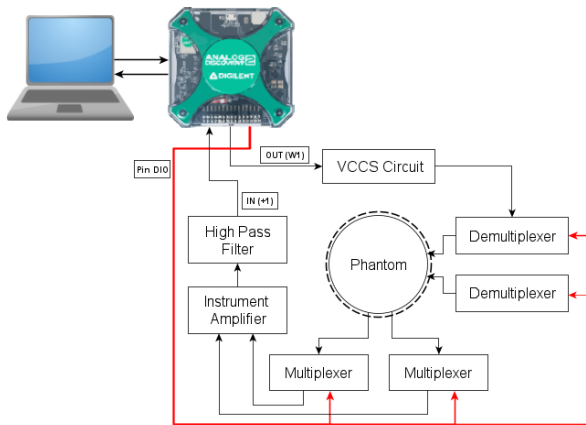
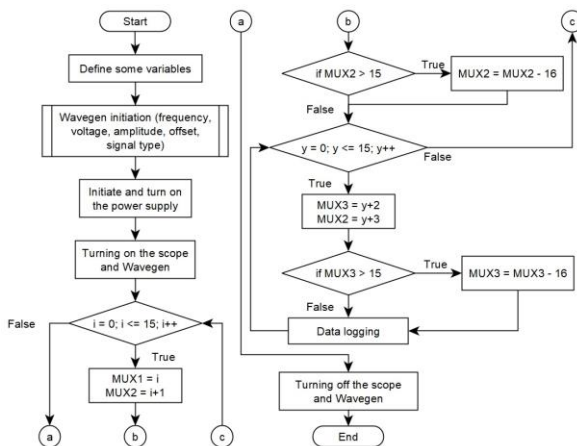**Figure 1** MfEIT design scheme to Detect Breast Cancer

Figure 2 MfEIT control flowchart based on Analog Discovery

The VCCS is a current source circuit by controlling the input voltage. The resulting current depends on the input voltage, according to equation (1) [27]. The VCCS circuit is built from IC OPA2134 and four 1 kΩ resistors, as shown in Figure 3. The VCCS test was carried out to determine its performance in maintaining the current generated against the given load. Testing VCCS was carried out at frequencies of 500 Hz, 1 kHz, 10 kHz, 40 kHz, 80 kHz and 100 kHz with loads of 100 Ω, 1 kΩ, 2 kΩ, 4 kΩ and 6 kΩ.
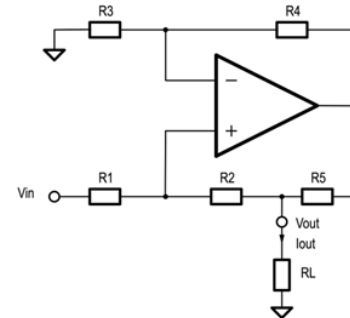

Figure 3 The VCCS circuit

$$I_{out} = -\frac{1}{R_4}\frac{R_3}{R_5}(V_{in}) \dots\dots\dots\dots\dots\dots(1)$$

The MfEIT device uses a multiplexer and demultiplexer of the IC74HC4067 module. Multiplexer and demultiplexer testing is carried out to identify whether the components are working according to the truth table. The multiplexer and demultiplexer in the MfEIT system to regulate the current, ground, and signal meter inputs.

The AD620 was used as an instrument amplifier which is useful for amplifying the differential signal measuring voltage between electrodes. The AD620 can amplify 1 to 10000 times by adding a resistor on the R_G pin according to Equation (2). The test was carried out by connecting a gain resistor (R_G) with a 50 kΩ potentiometer. The R_G was varied at 10 kΩ, 2 kΩ, 1 kΩ with frequencies at 500 Hz, 10 kHz, 20 kHz, 40 kHz and 80 kHz. The MfEIT system uses a high pass filter to pass high frequencies and remove low frequency signals from both DC signals and low frequency AC signals.

$$G = \frac{49{,}9k\Omega}{R_G} + 1 \dots\dots\dots\dots\dots\dots\dots\dots(2)$$

The phantom was used as a test object to know the performance of MfEIT in detecting breast anomalies. The breast phantom is from agar with a height of 4 cm, a diameter of 10.5 cm, and has a half-spherical shape. The phantom contains a cancer made of agar with a diameter of 1.4 cm. The phantom created has a conductivity of 0.06 S/m for breast tissue and 0.16 S/m for cancer tissue based on Equation 3 [28].

$$\sigma\left(S/m\right) = 215\ x\ \frac{(grams\ of\ NaCl)}{(solution\ volume, mL)} + 0.0529 ...(3)$$

The waveforms software control the Analog Discovery module to generate voltage signals, set up the multiplexer to measure voltage and demultiplexer to inject current, power supply as a resource for AD620, VCCS, multiplexer and demultiplexer.

Data collection was carried out with 16 electrodes from copper plates coded E-1, E-2, E-3 to E-16. All electrodes from E-1 to E-16 are connected to 2 demultiplexers and 2 multiplexers. The first demultiplexer is programmed to regulate the current injection position while the second demultiplexer is to regulate the ground position. The first and second multiplexers are used to set up voltage measurements on two adjacent electrodes.

Image reconstruction is carried out on voltage and phase data to produce the image being the distribution of the object's conductivity and its phases. Image reconstruction was carried out with EIDORS software using the relative imaging method of homogeneous and non-homogeneous data. EIDORS-V3.10 software was used for reconstruction image from voltage and phase measurement data. EIDORS is a MATLAB-based toolkit which includes several reconstruction methods and object shapes[26]. In this study, homogeneous data was obtained from the average of non-homogeneous data.

Analysis was carried out by comparing the reconstructed image on the phantom with anomalies and their placement and without anomalies between the image results with the phantom and the location of the anomalies. The correctness of the reconstruction results and how good the results obtained by the system created are by making visual observations between the location of the object, the number of anomalies in the phantom and the image reconstruction results of the program.

3.0 RESULT

All modules that make up the MfEIT device were carried out performance tests which included analog discovery, VCCS, multiplexer-demultiplexer, high pass filter, instrument amplifier, phantom, device integration, EIDORS reconstruction program, and data retrieval with phantom.

Analog Discovery's performance was tested for its ability to generate AC sine signals.

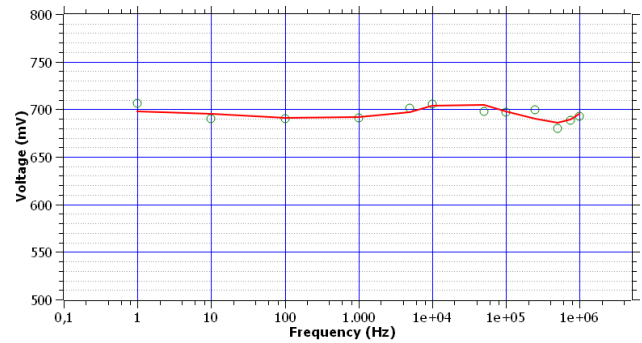Figure 4 is the resulting Vrms voltage, which is stable at 700 mV at a frequency of 1 Hz to 1 MHz.

Figure 4 Graph of Generator Signal Test

VCCS performance is stable at 0.3 mA, 0.29 mA, 0.284 mA, and 0.21 mA when given a load of 100 Ω, 1 kΩ, 4 kΩ and 6 kΩ, shown in Figure 5. Based on these results it can be said that the current value obtained is within safe limits if injected into the human body
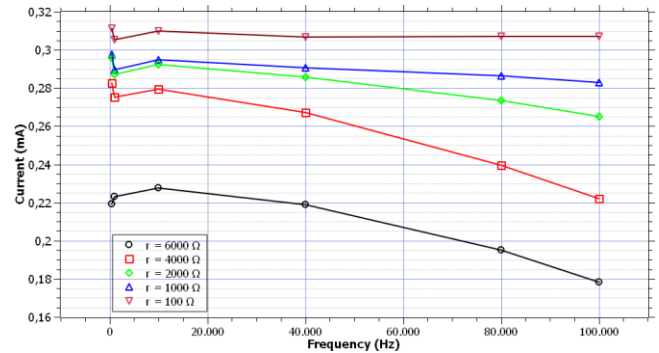
Figure 5 Graph of VCCS Test

Multiplexer and demultiplexer testing is carried out to ensure that the components used work properly according to the truth table. Tests were carried out on the IC 74HC4067 module and obtained the same results as in Table 1 which shows that all components are working well.

Table 1 The measurement results of IC 74HC40067 module

DIO 0	DIO 1	DIO 2	DIO 3	Output Active	DIO 0	DIO 1	DIO 2	DIO 3	Output Active
0	0	0	0	C0	1	0	0	0	C8
0	0	0	1	C1	1	0	0	1	C9
0	0	1	0	C2	1	0	1	0	C10
0	0	1	1	C3	1	0	1	1	C11
0	1	0	0	C4	1	1	0	0	C12
0	1	0	1	C5	1	1	0	1	C13
0	1	1	0	C6	1	1	1	0	C14
0	1	1	1	C7	1	1	1	1	C15

The performance of the high pass filter is shown in Figure 6. This filter design has a cut-off frequency of 159.15 Hz using a resistor of 1 kΩ and a capacitor of 1 µF.
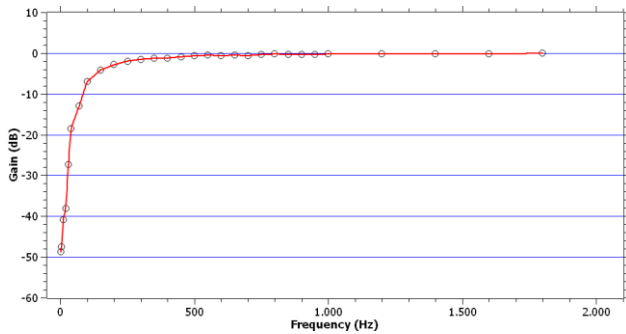

Figure 6 Graph of High Pass Filter Test

Instrument amplifier testing is carried out by providing a potentiometer load of 50 kΩ. The test was carried out 4 times, namely without loading, and varying loads of 10 kΩ, 2 kΩ, and 1 kΩ, by using equation 2, the respective Gains are G=1, G=5.94, G=25.7 and G=50.4. Tests were also carried out with frequency variations of 500 Hz, 10 kHz, 20 kHz, 40 kHz and 80 kHz. The results can be seen in Figure 7. The Gain is in accordance with the calculation in equation 2. However, the Gain calculation of 50.4 produces a smaller Gain. This shows the gain limit that can be obtained from the amplifier instrument. The gain used must be adjusted to the resistance of the phantom used, in this study it was found that the gain was 9.3 with a resistance of 6 kΩ.
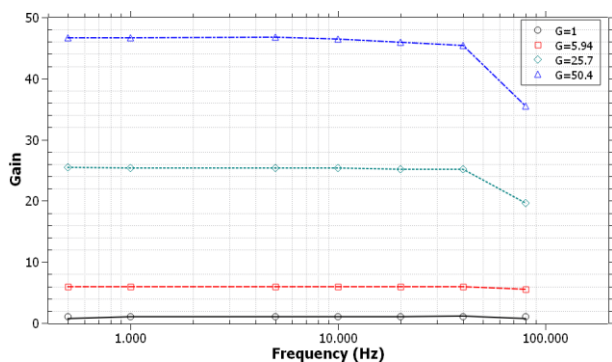
Figure 7 Graph of Instrument Amplifier Test

The breast phantom used in this study was made of agar with a height of 4 cm and a diameter of 10.5 cm, in the shape of a half ball. On the Phantom there is an artificial cancer which is also made of agar with a diameter of 1.4 cm. The phantom created has a conductivity value of 0.06 S/m for breast tissue and 0.16 S/m for cancer tissue. The phantoms is used by mixing 300 ml of water, 2.5 grams of agar and 0.15 grams of NaCl which is then heated for 1 minute while stirring, then poured into a mold. When it has

hardened it is cut into pieces with a diameter of 1.4 cm as cancer anomaly. Next, the same process is carried out but using 0.01 grams of NaCl, and pouring 200 ml into the mold and allowing it to harden, then placing the anomaly in the desired location and pouring 100 ml again as a second layer, this is done so that the anomaly can blend into the whole so that it resembles cancerous tissue in the breast. The phantom was created in two conditions, namely one anomaly and two anomalies as in Figure 8.
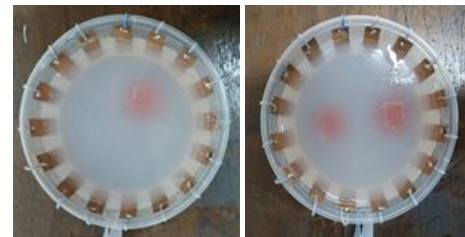

Figure 8 The phantom (a) one anomaly (b) two anomalies

After testing each module, a Printed Circuit Board (PCB) was then made to create Multifrequency Electrical Impedance Tomography (MfEIT).

Figure **9** shows the results of integrating all circuits on the PCB.

Figure 9 The MfEIT module system

EIDORS is a toolbox in the Matlab application that is used to reconstruct potential and phase data into images. EIDORS will read the data obtained in the form of .csv data which is then averaged as reference data. The FEM function program uses the size g2d1c, namely 3136 triangular elements and 1 distmesh. The GN_one_step method is used with hyperparameters of 0.005.

Data collection was carried out on a phantom with 16 electrodes with a current of 0.29 mA. Data collection was carried out once for each phantom with 3 different frequencies, namely at frequencies of 10 kHz, 40 kHz and 80 kHz, so that a total of 6 data were obtained with details of 3 voltage data and 3 phase data for each phantom. Figure 10 is one of the potential and phase raw data produced by this MfEIT device.
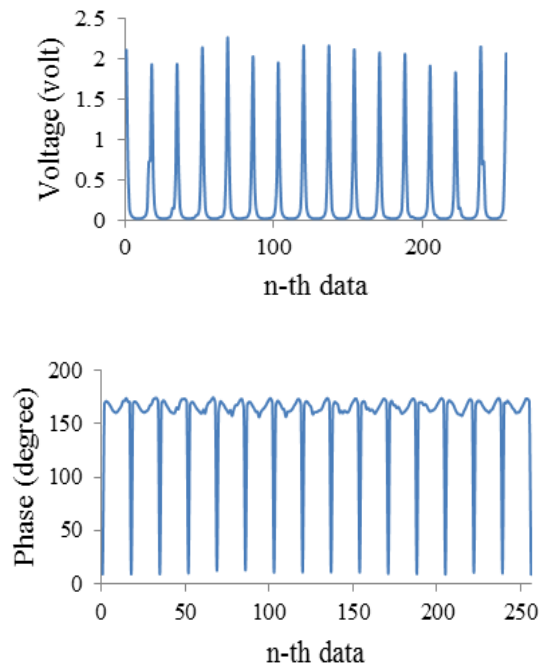
Figure 10 The raw data produced by MfEIT (a) Potential (b) Phase

The reconstruction of potential and phase data from one and two anomalies was shown in Table 2 and Table 3 respectively. Table 2 show the phantom one anomaly with a hyperparameter of 0.005 which shows that there is an anomaly in the form of a red color with high contrast to its surroundings. The red color is an anomaly because in the EIDORS program the blue area shows a lower conductivity distribution value and red for the area greater conductivity, because cancer has higher conductivity so it appears red compared to the surrounding area [16]. When compared with the original placement, both the voltage data and phase data both show anomalies with the same location on the phantom, namely around the 14th and 15th electrodes at frequencies of 10 kHz, 40 kHz and 80 kHz. However, at a frequency of 80 kHz, the location of the anomaly appears to be slightly shifted compared to other frequencies.

Table 3 shows the results of image reconstruction on a phantom with two anomalies. Just like in the phantom with one anomaly, two red anomalies were found in both the voltage data and the phase data. The location of the anomaly also looks exactly like the location of the original anomaly at both frequencies of 10 kHz and 40 kHz. However, at 80 kHz it appears that the location of the anomaly has shifted slightly and in the phase data only one anomaly can be detected. The other anomaly is less readable due to the process of making the anomaly, the solution was not stirred evenly so that anomalies 1 and 2 are not compositionally symmetrical, so that anomaly 2 is less readable.

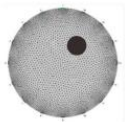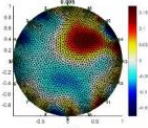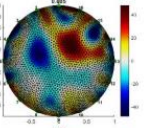**Table 2** The one anomaly phantom and reconstruction image
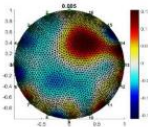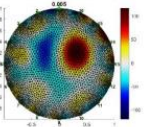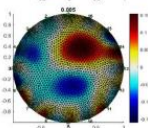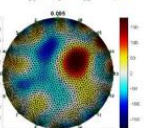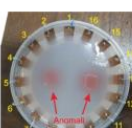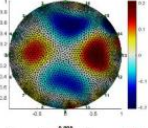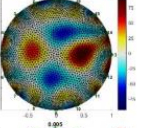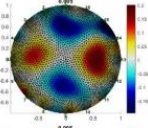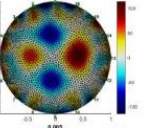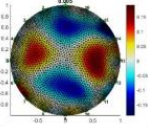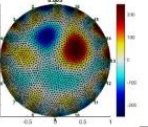
Table 3 The two anomaly phantom and reconstruction image

The reconstructed image contains noise in the form of blue which should not be there, but this can be adjusted by increasing/decreasing the hyperparameter value. The blue to red color in other areas, especially in the edge areas, is noise from the measurement results caused by electrodes that are too close and can also be caused by other substances mixed in the phantom or because the phantom was not stirred enough during the manufacturing process, as well as due to reconstruction.

Based on the results of the reconstruction that has been carried out, it can be seen that the Multifrequency Electrical Impedance Tomography (MfEIT) that has been built is capable of detecting anomalies in phantoms made with either one anomaly or two anomalies. The reconstructed image looks better when using a hyperparameter of 0.005. From the results obtained, it can be seen that the image results can be seen clearly and in contrast, both in the voltage data and in the phase difference data, with the position corresponding to the original anomaly placement. The image results also show that the image looks better at frequencies less than

80 kHz for phase difference data because at high frequencies there are deviations in the location of anomalies.

5.0 CONCLUSION

Multifrequency Electrical Impedance Tomography (MfEIT) can be built from Analog Discovery which can be used as a signal generator, power supply, voltage control and data acquisition resulting from measurements of voltage and phase difference data from a breast phantom made of agar. This device can produce a stable electric current of 0.29 mA.

Image reconstruction using EIDORS software from the Electrical Impedance Tomography (EIT) system which is made capable of detecting anomalies in both voltage data and phase difference data, with a hyperparameter of 0.005 to detect anomalies. The reconstructed image shows that there is an anomaly that has higher conductivity which is represented in red and the surrounding area tends to be colored blue. The image reconstruction results appear clear in the frequency range of 10 kHz to 80 kHz for voltage data, and at frequencies of 10 kHz to 40 kHz for phase difference data.

Acknowledgement

Conflict of interest

All authors declare that they have no conflicts of interest.

References

[1] Hero, S. K. 2021. Faktor Resiko Kanker Payudara. *Jurnal Medika Hutama.* 03(01): 1533–1537. [Online]. Available: https://jurnalmedikahutama.com/index.php/JMH/article/view/310/212.

[2] Fass L. 2008. Imaging and Cancer: A Review. *Moecular Oncoogyl.* 2(2): 115–152. Doi: 10.1016/j.molonc.2008.04.001.

[3] American Cancer Society. 2021. About Breast Cancer. https://www.cancer.org/content/dam/CRC/PDF/Public/8577.00.pdf (accessed Sep. 21, 2023).

[4] Widyawati. 2022. Kanker Payudara Paling Banyak di Indonesia, Kemenkes Targetkan Pemerataan Layanan Kesehatan. Ministry of Health. https://sehatnegeriku.kemkes.go.id/baca/umum/20220202/1639254/kanker-payudaya-paling-banyak-di-indonesia-kemenkes-targetkan-pemerataan-layanan-kesehatan/ (accessed Sep. 25, 2023).

[5] Karellas, A. and Vedantham, S. 2008. Breast Cancer Imaging: A Perspective for the Next Decade. *Med. Phys.* 35(11): 4878–4897. Doi: 10.1118/1.2986144.

[6] Jaglan, P., Dass, R. and Duhan, M. 2019. Breast Cancer Detection Techniques: Issues and Challenges. *J. Inst. Eng. Ser. B.* 100(4): 379–386. Doi: 10.1007/s40031-019-00391-2.

[7] Zavare, M. A. and Latiff, L. A. 2015. Electrical Impedance Tomography as a Primary Screening Technique for Breast Cancer Detection. *Asian Pacific J. Cancer Prev.* 16(14): 5595–5597. Doi: 10.7314/APJCP.2015.16.14.5595.

[8] Chakraborti, D. K. L. and Selvamurthy, D. W. 2010. Clinical Application of Electrical Impedance Tomography in the Present Health Scenario of India. *J. Phys. Conf. Ser.* 224: 012069. Doi: 10.1088/1742-6596/224/1/012069.

[9] Zain, N. M. and Chelliah, K. K. 2014. Breast Imaging Using Electrical Impedance Tomography: Correlation of Quantitative Assessment with Visual Interpretation. *Asian Pacific J. Cancer Prev.* 15(3): 1327–1331. Doi: 10.7314/APJCP.2014.15.3.1327.

[10] Disha, E.D., Kërliu, S.M., Ymeri, H. and Kutllovci, A. 2009. Comparative Accuracy of Mammography and Ultrasound in Women with Breast Symptoms According to Age and Breast Density. *Bosn. J. Basic Med. Sci.* 9(2): 131–136. Doi: 10.17305/bjbms.2009.2832.

[11] Zarafshani, A., Huber, N., Beqo, N., Tunstall, B., Sze, G., Chatwin, C. And Wang, W. 2010. A Flexible Low-cost, High-precision, Single Interface Electrical Impedance Tomography System for Breast Cancer Detection using FPGA. *J. Phys. Conf. Ser.* 224: 012169. Doi: 10.1088/1742-6596/224/1/012169.

[12] Khan, T. A. and Ling, S. H. 2019. Review on Electrical Impedance Tomography: Artificial Intelligence Methods and its Applications. *Algorithms.* 12(5): 88. Doi: 10.3390/a12050088.

[13] Wu, H., Zhou, W., Yang, Y., Jia, J. and Bagnaninchi, P. 2018. Exploring the Potential of Electrical Impedance Tomography for Tissue Engineering Applications. *Materials (Basel).* 11(6): 930. Doi: 10.3390/ma11060930.

[14] Saulnier, G. J., Blue, R. S. , Newell, J. C., Isaacson, D. and Edic, P. M. 2001. Electrical Impedance Tomography. *IEEE Signal Process. Mag.* 18(6): 31–43. Doi: 10.1109/79.962276.

[15] Lee, E., Erdene, M., Seo, J. K. and Woo, E. J. 2012. Breast EIT using a New Projected Image Reconstruction Method with Multi-frequency Measurements. *Physiol. Meas.* 33(5): 751–765. Doi: 10.1088/0967-3334/33/5/751.

[16] Qiao, G., Wang, W., Wang, L., He, Y., Bramer, B. and Al-Akaidi, M. 2007. Investigation of Biological Phantom for 2D and 3D Breast EIT images. *13th International Conference on Electrical Bioimpedance and the 8th Conference on Electrical Impedance Tomography.* 328–331. Doi: 10.1007/978-3-540-73841-1_86.

[17] Pennati, F., Angelucci, A., Morelli, L., Bandini, S., Barzanti, E., Cavallini, F., Conelli, A., Federico, G., Paganelli, C. And Aliverti, A. 2023. Electrical Impedance Tomography: From the Traditional Design to the Novel Frontier of Wearables. *Sensors.* 23(3): 1182. Doi: 10.3390/s23031182.

[18] Zain, N. M., Kanaga, K. C., Sharifah, M. I. A., Suraya, A. and Latar, N. H. 2014. Study of Electrical Impedance Tomography as a primary screening technique for breast cancer. *2014 IEEE Conference on Biomedical Engineering and Sciences (IECBES).* 220–224. Doi: 10.1109/IECBES.2014.7047490.

[19] Juliana, N., Shahar, S., Chelliah, K. K., Ghazali, A. R., Osman, F. and Sahar, M. A. 2014. Validation of Electrical Impedance Tomography Qualitative and Quantitative Values and Comparison of the Numeric Pain Distress Score against Mammography. *Asian Pacific J. Cancer Prev* 15(14): 5759–5765. Doi: 10.7314/APJCP.2014.15.14.5759.

[20] Dabacan, M. 2018. Analog Discovery 2 Reference Manual. *Analog Discov. 2 Ref. Manual-Digilent Ref.* [Online]. Available: http://autolab.sjtu.edu.cn/Assets/userfiles/sys_eb538c1c-65ff-4e82-8e6a-a1ef01127fed/files/AD2用户手册.pdf.

[21] Ain, K., Putra, A. P., Rahma, O.n., Hikmawati, D., Rahmatillah, A., and Abdullah, C. A. 2024. Electrical Impedance Spectroscopy as a Potential Tool for

Detecting Bone Porosity. *Sensors and Actuators: A. Physical*. 370. https://doi.org/10.1016/j.sna.2024.115252.

[22] Sapuan, I., Ain, K. and Suryanto, A. 2017. Dual Frequency Electrical Impedance Tomography to Obtain Functional Image. *J. Phys. Conf. Ser*. 853(1): 012002. Doi: 10.1088/1742-6596/853/1/012002.

[23] Trokhanova, O. V., Okhapkin, M. B. and Korjenevsky, A. V. 2008. Dual-frequency Electrical Impedance Mammography for the Diagnosis Oof Non-malignant Breast Disease. *Physiol. Meas*. 29(6): S331–S344. Doi: 10.1088/0967-3334/29/6/S28.

[24] Ain, K., Kurniadi, D., Ulum, M. F., Choridah, L., Mukhayyar, U., Garnadi, A. D., Setyawan, N. H., Ariwanto, B. 2022. Development of Multi Frequency Electrical Impedance Tomography For Rectangular Geometry by Finite Volume Methods. *Jurnal Teknologi*. 84(2): 9–15. Doi: 10.11113/jurnalteknologi.v84.16936.

[25] Cortes, J. C. G., Olivarez, J. P., Carmona, J. J. D., Medina, J. A. P., Munoz, J. A. G. and Gutierrez, A. I. B. 2022. Electrical Impedance Tomography Simulation for Detection of Breast Tumors Based on Tumor Emulators. *45th International Conference on Telecommunications and Signal Processing (TSP)*. 395–398. Doi: 10.1109/TSP55681.2022.9851291.

[26] Mikulka, J., Zimniok, D. and Dušek, J. 2023. Laboratory System of Electrical Impedance Tomography. *14th International Conference on Measurement*. 71–74. Doi: 10.23919/MEASUREMENT59122.2023.10164432.

[27] Batista, D. S., Granziera, F., Tosin, M. C., de Melo, L. F. 2023. Analysis and Practical Implementation of a High-power Howland Current Source. *Measurement*. 297: 1–11. https://doi.org/10.1016/j.measurement.2022.112404.

[28] Bennett, D. 2011. NaCl Doping and the Conductivity of Agar Phantoms. *Materials Science and Engineering: C*. 31(2): 494–498. Doi:10.1016/j.msec.2010.08.018.